ACTA RADIOLOGICA

OFFICIAL ORGAN OF THE RADIOLOGICAL SOCIETIES OF
DENMARK, FINLAND, NORWAY AND SWEDEN

Vol. 11 Fasc. 2 — THERAPY PHYSICS BIOLOGY — 1972 April

CORRECTION OF ISODOSE-DIAGRAMS FOR ^{60}Co AND 35 MeV ELECTRONS AT PENETRATION OF LUNG TISSUE

by

ULLA-BRITA NORDBERG

Measurements in a phantom were made to investigate how the course of isodose curves is influenced by the passage of regions having a volume weight of less than 1 g/cm^3. This effect is correlated to volume weight to enable a simple, approximate calculation of the corrections necessary in routine dose planning. The individual volume weight of normal lung tissue was established for 13 patients.

Material. The thorax phantom consisted entirely of polystyren. On the entrance side there was a 3 cm thick homogeneous sheet corresponding to the thorax wall, and then 3 mm polystyren sheets perforated with holes 3 mm in diameter, simulating lung tissue. The sheets were stratified so that small air-bubbles of about 3 mm in diameter were formed. Human lung tissue contains alveoli, the diameter of which can be up to 1 mm at the most. The phantom had the same chemical composition in its homogeneous part as in its lung simulating part, though in the latter the volume weight (in g/cm^3) was lower. Lung volume weight was varied by introducing 1 mm air-gaps, respectively 1 mm homogeneous sheets between the perforated polystyren sheets, thus getting

From the Department of Radiation Physics (Director: Prof. K. Lidén), University of Lund, Sweden. Submitted for publication 12 March 1971.

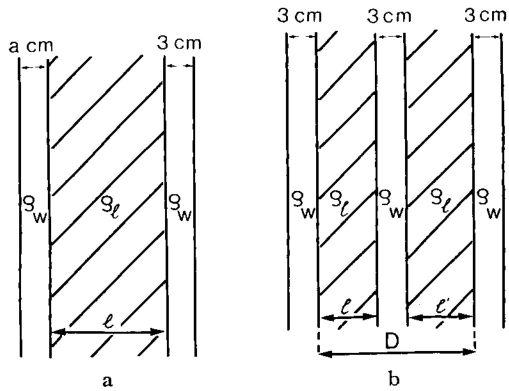

Fig. 1. Thorax phantom constructions. a) ϱ_w = 1.04 g/cm³. Phantoms A, B, C and D, a = 3 cm, l = 20, 15, 9 and 3 cm, ϱ_l = 0.58, 0.42, 0.32 and 0.25 g/cm³. Phantom G, a = 1.5 cm, l = 20 cm, ϱ_l = 0.42 g/cm³. b) ϱ_w = 1.04 g/cm³, ϱ_l = 0.42 g/cm³. Phantom E, D = 20 cm, l = 10 cm, l' = 7 cm. Phantom F, D = 13 cm, l = 6 cm, l' = 4 cm.

volume weights (ϱ_l) of 0.32, 0.42 and 0.58 g/cm³. For some of the measurements the lung simulating part was made of sawdust, compressed to a volume weight of 0.25 g/cm³.

The phantom measurements were made with microionization chambers and with photographic film. Certain measurements referred to were made in a water phantom with a cable-connected ionchamber or with Fricke dosimeters. Calculation of absorbed dose from measured ionization for electrons was done by means of a calibration curve drawn from identical depth dose determinations with ionchambers and Fricke dosimeters. The mean electron energy E_x at a depth of x g/cm² is assumed to be (E_0 — k x) MeV, where E_0 is the initial electron energy in MeV and $k = 2$ MeV/1 cm.

The wall of the microionization chambers was about 0.25 g/cm² and required a perspex cap for exposure measurements with ^{60}Co radiation. A number of chambers provided with caps 0, 0.5, 1.0, 2.0, 2.5 and 3.0 mm thick were irradiated in a thorax phantom having a volume weight of 0.25 g/cm³. The absorbed dose was evaluated using the individual chamber constants valid for a 3.0 mm cap. Investigations were made in the thorax phantom at depths of 2.5, 5.0 and 10.0 cm. Absorbed dose determinations with different cap thicknesses were, at all the depths, within ± 3 % for 14 measuring chambers at each depth. As a result, no caps were used for the measurements in the thorax phantom.

Method

Cobalt-60. The central axis depth absorbed dose for the field 10 cm × 10 cm at SSD 70 cm was determined with ionchambers for four different types of phantom (A, B, C, D) and for four different lung volume weights (1, 2, 3, 4) (Fig. 1 a).

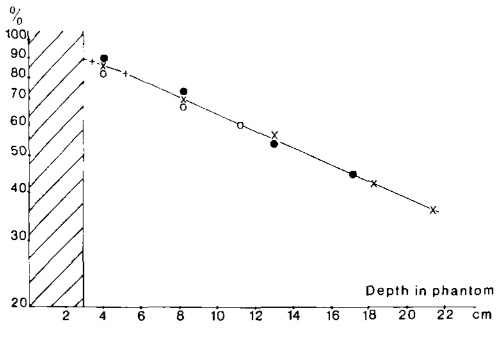

Fig. 2. Central axis depth absorbed dose in the phantoms A, B, C and D: ^{60}Co, SSD 70 cm, 10 cm × 10 cm, ϱ_l = 0.42 g/cm³. Measurement in phantom A (×), B (●), C (○) and D (+).

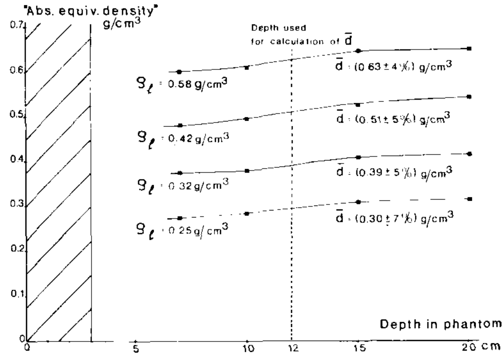

Fig. 3. 'Absorbed equivalent density' (d) as a function of depth in phantom for different ϱ_l. $\bar{d}$ = mean value of d in the investigated interval.

The four phantom types were: (A) 3 cm thorax wall (volume weight ϱ_w = 1.04 g/cm³), 20 cm lung tissue, 3 cm thorax wall; (B) the same as (A), but with 15 cm lung tissue; (C) the same as (A), but with 9 cm lung tissue; (D) the same as (A), but with 3 cm lung tissue.

The four lung volume weights (ϱ_l) were: (1) 0.58 g/cm³; (2) 0.42 g/cm³; (3) 0.32 g/cm³; (4) 0.25 g/cm³.

Measurements were not made within the thorax walls themselves nor close to the border-lines between different volume weights.

The absorbed dose distribution perpendicular to the central axis was determined at 6, 10 and 14 cm depths in the thorax phantom with a volume weight of 0.42 g/cm³. The same distribution has also been measured in a water-equivalent phantom at depths having the same central axis depth absorbed dose as 6, 10 and 14 cm in the thorax phantom. Ionization chambers were used for these measurements.

35 MeV electrons. The central axis depth absorbed dose for the field 10 cm × 8 cm at SSD 110 cm was determined with ionchambers for four different phantom variants and three different lung volume weights. The four phantom

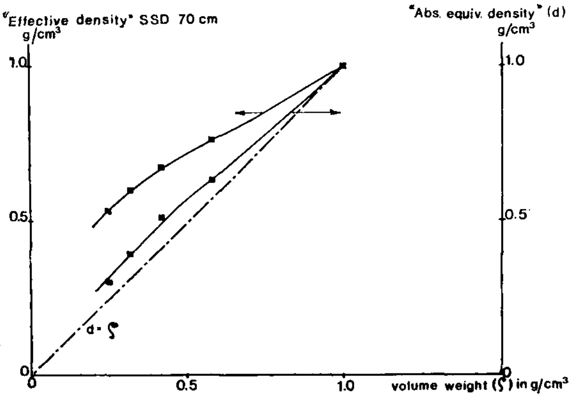

Fig. 4. 'Effective density' (d') for SSD 70 cm (left curve) and 'absorption equivalent density' (d, right curve) as functions of volume weight (ϱ_l) for ^{60}Co.

types were the same as for the ^{60}Co measurements. The depth absorbed dose for the same radiation geometry was determined for one lung volume weight (0.42 g/cm^3) in two phantom types (E and F) where an extra wall of water-equivalent material was placed at different depths in the lung tissue (Fig. 1 b): (E) 3 cm thorax wall, 10 cm lung tissue, 3 cm extra wall, 7 cm lung tissue, 3 cm thorax wall; (F) 3 cm thorax wall, 6 cm lung tissue, 3 cm extra wall, 4 cm lung tissue, 3 cm thorax wall.

Also the depth absorbed dose for one lung volume weight (0.42 g/cm^3) was established in a phantom where the anterior thorax wall was only 1.5 cm thick (G in Fig. 1 a): (G) 1.5 cm thorax wall, 20 cm lung tissue, 3 cm thorax wall.

Measurements were not made close to the border-lines between two volume weights.

The absorbed dose distribution perpendicular to the central axis at a depth of 13 cm in the thorax phantom with lung volume weight 0.42 g/cm^3 was investigated using film, the optical density of which was evaluated in per cent of the density in the central axis. The density of the film has earlier been proved to be linearly dependent on the absorbed dose in corresponding measurements with film in homogeneous phantom, where film density was correlated with depth absorbed dose measurements.

Results

Cobalt-60. Fig. 2 gives the ^{60}Co measurements in the four different phantom types (A, B, C, D) for volume weight 0.42 g/cm^3. Due to the measuring errors, only one curve can be drawn, which implies that the absorbed dose at a point in the lung tissue is largely independent of the amount of lung tissue behind it. This is also valid for the other volume weights. When x cm of a material,

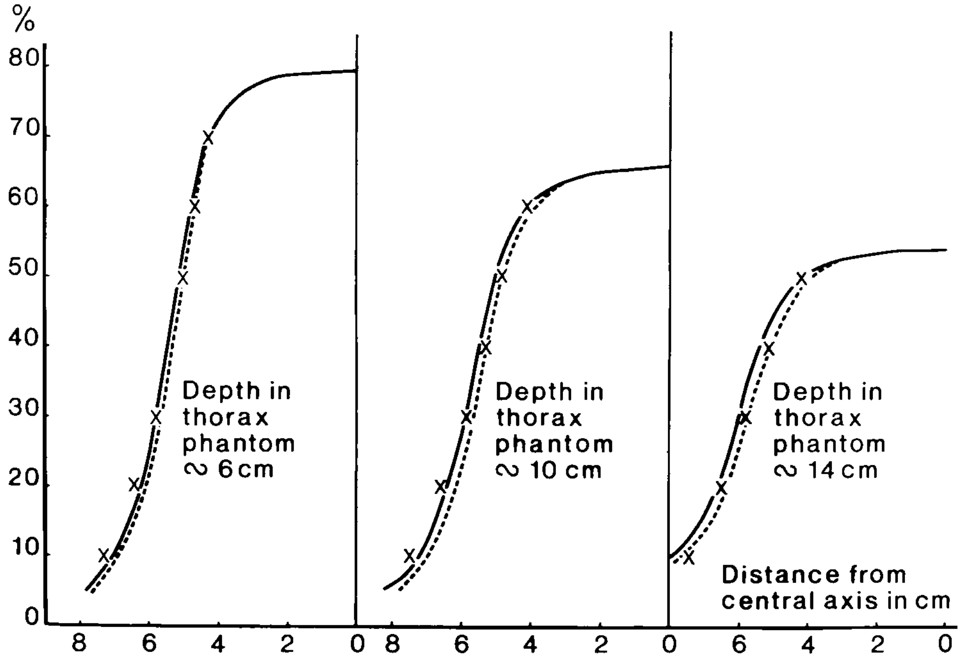

Fig. 5. Absorbed dose distribution perpendicular to central axis. ^{60}Co, SSD 70 cm, 10 cm × 10 cm, $\varrho_l = 0.42$ g/cm³. Measuring points in thorax phantom (×), distribution in water-equivalent material corrected for increased depth (full-drawn curve); the same distribution without this correction (dotted curve).

measured along the central axis with broad beam geometry in a phantom, causes the same decrease in depth absorbed dose as y cm of water with density ϱ_{H_2O} g/cm³, the value $y/x \cdot \varrho_{H_2O}$ g/cm³ in this paper will be used as the 'effective density' of the material, valid for the SSD used. If the radiation beam is parallel, the value $y/x \cdot \varrho_{H_2O}$g/cm³ will be named 'absorption equivalent density'. The inverse square law effect for the valid SSD and for the depth differences between x and y can be eliminated. Thus, the 'effective density' can be converted into an 'absorption equivalent density' independent of SSD.

Comparing the measured values from Fig. 2 with the corresponding central axis data from the Brit. J. Radiol. Sûppl. No. 10 for water, an 'effective lung density' valid for SSD 70 cm is obtained. A calculation of an 'absorption equivalent density' is done for four different depths. Fig. 3 shows that the 'absorption equivalent density' (d) is almost constant, regardless of the depth for which the value is calculated. Fig. 4 shows the mean value of this 'density' ($\bar{d}$, corresponding to the value at a depth of 12 cm in Fig. 3) as a function of the true volume weight. In the diagram there is also a curve with the 'effective

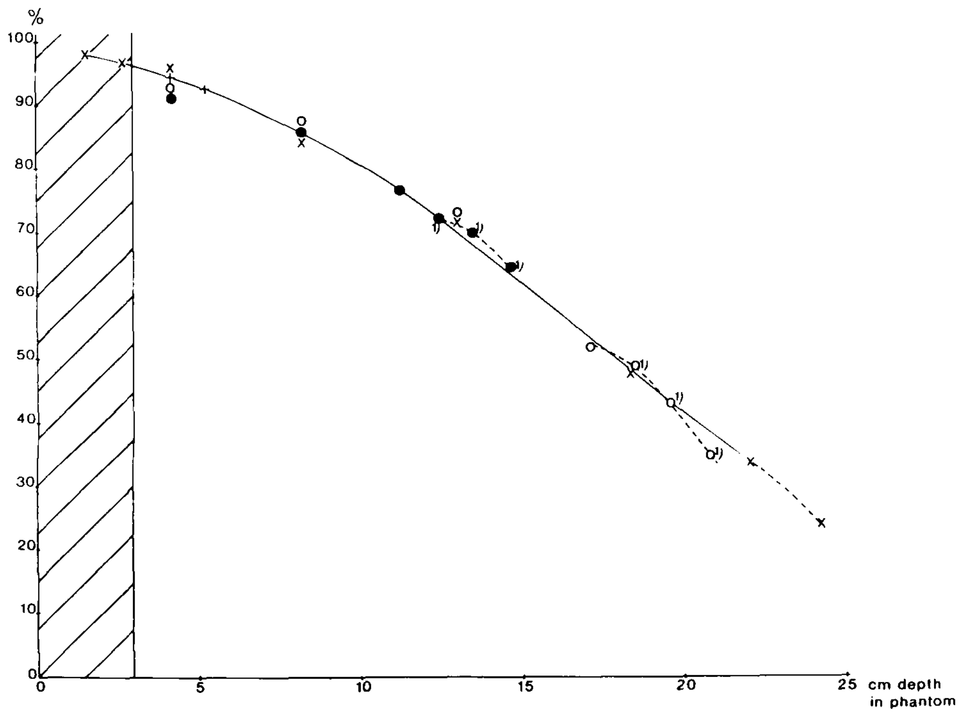

Fig. 6. Central axis depth absorbed dose in thorax phantoms A, B, C and D: 35 MeV e⁻, SSD 110 cm, 10 cm × 8 cm, ϱ_l = 0.42 g/cm³. Measurements in phantom A (×), B (○), C (●) and D (+). Measurements marked 1) were made in the posterior chest wall. Mean value of measurement in lung (full-drawn curve).

density' valid for SSD 70 cm, as a function of the true volume weight. This 'effective density', arrived at directly from the slope of the depth absorbed dose curve in lung tissue, is the one which is determined at individual exit measurements on patients.

Fig. 5 shows the absorbed dose distribution perpendicular to the central axis for depths of 6, 10 and 14 cm in the lung phantom, ($\varrho_l = 0.42$ g/cm³), as well as corresponding distribution in water-equivalent phantom at levels having the same depth absorbed dose in the central axis. If a correction for divergence of the latter distribution to corresponding depths in the lung phantom is done, a somewhat wider (2—4 mm) distribution is obtained. The water and lung curves are considered to be in agreement within the measuring errors.

35 MeV electrons. Fig. 6 shows the central axis depth absorbed dose for the field 10 cm × 8 cm at SSD 110 cm, volume weight 0.42 g/cm³ and different phantom types (A, B, C, D). The spread in the measuring values for the different

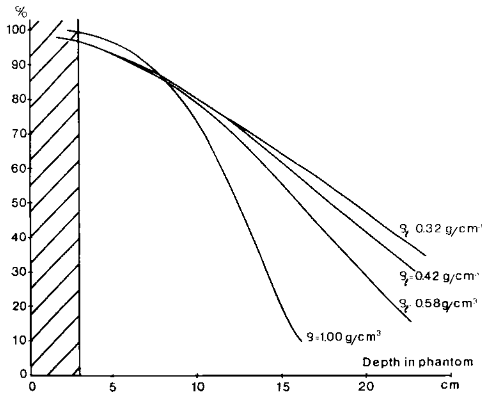

Fig. 7

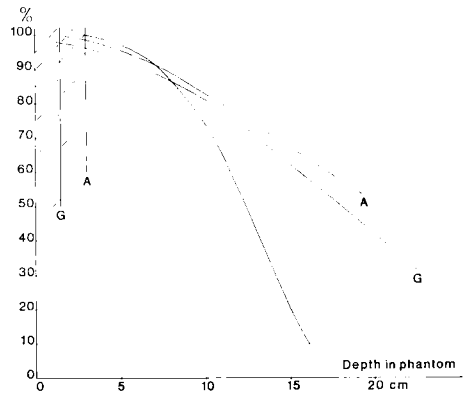

Fig. 8

Fig. 7. Central axis depth absorbed dose in thorax phantom: 35 MeV e⁻, SSD 110 cm, 10 cm × 8 cm, ϱ_l = 0.58, 0.42 and 0.32 g/cm³. ϱ_l = 1.00 g/cm³ indicates corresponding water curve.

Fig. 8. Central axis depth absorbed dose in thorax phantom: 35 MeV e⁻, SSD 110 cm, 10 cm × 8 cm, ϱ_l = 0.42 g/cm³. Phantoms A and G.

phantom types is greater here than with ^{60}Co. A mean value curve of the lung measurements was drawn which is later used. The dotted parts of the curve show the course in the posterior thorax wall for the three largest phantom types. The increase in depth absorbed dose immediately within the posterior wall is due to build-up of δ-particles and the decrease at the exit side is due to lack of back-scattered electrons. There is a corresponding relation for the other two volume weights.

Fig. 7 shows the mean value curve from Fig. 6, together with the corresponding mean value curves for volume weights 0.32 and 0.58 g/cm³, and the depth absorbed dose curve in water, obtained with Fricke dosimeters, the curves being normalized to the same incident electron fluence. The absorbed dose in the anterior chest wall and in the 'lung' immediately behind this wall was found to be lower than it would be in a homogeneous water equivalent phantom, due to lack of back-scattered electrons. At about 5 cm depth in lung tissue, the absorbed dose in the thorax phantom became higher than the absorbed dose in water at the same depth.

Fig. 8 shows the depth absorbed dose for volume weight 0.42 g/cm³ with anterior thorax wall 1.5 and 3 cm, respectively. The curves belonging to the different thicknesses have about the same shape.

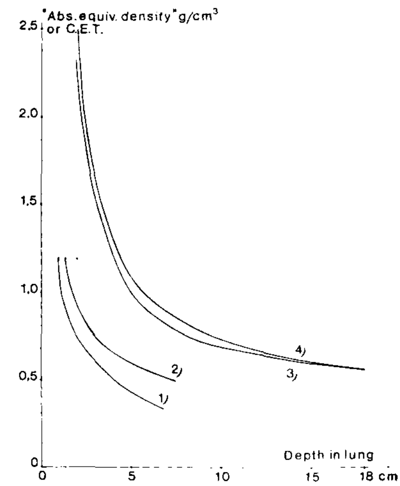

Fig. 9. 'Absorption equivalent density' (or CET) as a function of depth in lung. 1) 2 cm chest wall, 9 MeV e⁻, $\varrho_l = 0.39$ g/cm³, (ALMOND et coll.), 2) 2 cm chest wall, 15 MeV e⁻, $\varrho_l = 0.39$ g/cm³, (ALMOND et coll.), 3) 3 cm chest wall, 35 MeV e⁻, $\varrho_l = 0.42$ g/cm³ (present investigation), 4) 1.5 cm chest wall, 35 MeV e⁻, $\varrho_l = 0.42$ g/cm³, (present investigation).

ALMOND et coll. (1967) have made similar depth absorbed dose measurements in lung tissue for up to 18 MeV electrons, using a thorax wall of 2 cm (in a few cases 4 cm) together with a true lung volume weight of 0.39 g/cm^3. The value 0.39 g/cm^3 may practically be considered as comparable to 0.42 g/cm^3 in the present investigation, which is the volume weight of the phantom consisting only of perforated sheets. These depth absorbed doses show the same reduction in relation to water curves at small depths, but the deviations are less, and extend only about 1.5 cm into the lung tissue.

The depth absorbed dose from the thorax phantom was compared with corresponding values for water equivalent material at different depths. As for ^{60}Co, the effect of inverse square law was eliminated. The 'absorption equivalent density' for volume weight 0.42 g/cm^3 thus calculated for different depths is shown in Fig. 9 as a function of depth in lung tissue together with corresponding results by ALMOND et coll. (1967). ALMOND et coll. and BOONE et coll. (1969) use the expression 'coefficient of equivalent thickness' (CET), which corresponds to the numerical value of the virtual 'absorption equivalent'. This is greater than 1 g/cm^3 for depths smaller than the depth where the water and lung curves cross each other (see Discussion). The thin wall gives somewhat higher value than the thick wall, which has also been accounted for by ALMOND et coll.

The perpendicular absorbed dose distribution at a depth of 6, respectively 10 cm lung tissue (that is 9, respectively 13 cm depth in the phantom) is seen in Fig. 10. The distribution in water equivalent material at levels with about

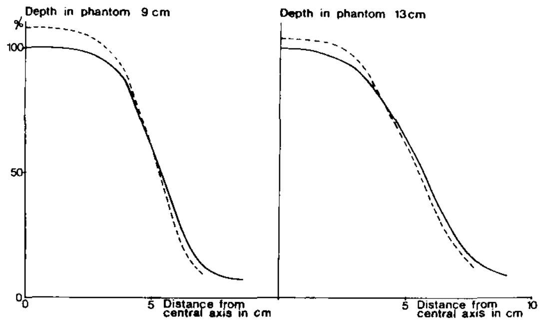

Fig. 10. Absorbed dose distribution perpendicular to central axis, 35 MeV e^-, SSD 110 cm, 10 cm × 8 cm, ϱ_l = 0.42 g/cm^3. Full-drawn curve indicates measured and dashed curve calculated values without correction for divergence.

the same depth absorbed dose at the central axis is also given here. Motivation for choosing these levels is presented later on in this paper. The correction for divergence is unimportant and may be ignored. The deviations within the penumbra region can be considered as small, for clinical purposes. The distribution in lung tissue is largely unchanged if the posterior thorax wall lies immediately behind the measuring plane or 10 cm away.

Discussion

For ^{60}Co, the primary absorbed dose contribution at a point in thorax can be calculated from the depth in g/cm^2 using true lung volume weight, together with inverse square law correction for the difference between the true depth and the corresponding depth in water. The scatter contribution to the same point decreases with density and the attenuation of this contribution is diminished. The net effect is negative. This decrease in scattering contribution results in a lower total depth absorbed dose than would be expected from depth in g/cm^2 using true lung volume weight. The correction for inverse square law has the same effect. This corresponds to a virtual density greater than the true volume weight. In this investigation the virtual density arrived at directly from measurements is called 'effective density'. If the effect of inverse square law is eliminated, it is called 'absorption equivalent density'.

The depth absorbed dose increases with enlarged field size, that is increased scatter contribution. For ^{60}Co the depth absorbed dose increases for example from 16 cm^2 field to 100 cm^2 field 5, 10 and 15 % at 4, 8 and 12 cm, respectively. Foı 35 MeV electrons, the corresponding increase is 4, 26 and 75 %.

It seems reasonable to assume that the ratio between 'absorption equivalent density' and volume weight is near to 1 for small scatter contribution. That is, for cobalt, 'absorption equivalent density' ought to be near the true volume weight and be relatively independent of the depth, while for electrons a greater and variable difference would be expected.

Cobalt-60. Fig. 3 confirms that the 'absorption equivalent density' for ^{60}Co is largely independent of the depth for a given volume weight. The ratio between the 'absorption equivalent density' and the volume weight varies according to the left part of Fig. 5 for ^{60}Co between 1.07 and 1.20 within the interval investigated.

The scatter contribution was calculated for the different volume weights from the measured depth absorbed dose curve at 12 cm depth, that is at 9 cm depth in the lung tissue. This contribution varied from 72 to 83 % of the corresponding contribution in water phantom. In order to see the reduction in direct relation to the volume weight, the same calculations were made for the same depths in g/cm^2 (6.8 g/cm^2). The scatter contribution then varied from 60 to 90 % of the corresponding contribution in water phantom for change of volume weight from 0.25 to 0.58 g/cm^3.

The value of volume weight for normal lung tissue given by different authors varies between 0.2 and 0.4 g/cm^3 (1, 3, 6, 7, 8, 9, 11). However, patients who are irradiated in the thorax region often have abnormal lung volume weight.

Measurements on 13 patients with roentgenologically unaffected lung gave 'effective densities' for SSD 70 cm from 0.41—0.74 g/cm^3, mean value 0.55 g/cm^3. According to Fig. 4, this corresponds to a volume weight of 0.27 g/cm^3, which value is in agreement with DAHL & VIKTERLÖF's (1955) measurements on calf lung.

In order to correct the absorbed dose of a cobalt treatment according to exit measurements, it is not necessary to know the true volume weight of the lung. If, however, such measurements have to be transferred to treatment with another type of irradiation where exit measurements can hardly be done, for example with electrons, it may be necessary to calculate the true volume weight.

35 MeV electrons. Fig. 9 confirms that for 35 MeV electrons, the ratio between 'absorption equivalent density' and volume weight in a thorax phantom varies considerably and is much higher than for ^{60}Co. For volume weight 0.42 g/cm^3 it varies from 2.4 to 1.3 between 5 and 20 cm depth in lung tissue. Measurements for 15 MeV electrons by ALMOND et coll. (1967) give values between 2.8 and 1.3 in the interval 1.5 to 7.5 cm depth in lung tissue. LAUGHLIN (1965) has suggested an 'absorption equivalent density' of 0.5 g/cm^3 for normal lung tissue and for 22 MeV electrons (valid for different depths and field sizes) and volume weight 0.33 g/cm^3, that is a ratio of 1.5. LAUGHLIN (1965) also has used a factor of 1.3 together with a volume weight of 0.38 g/cm^3, which means the same value of 0.5 g/cm^3 for 'absorption equivalent density'. DAHLER et coll. (1969) also recommended this ratio. POHLIT (1969) suggested a depth absorbed dose shift, which gives the ratio of 1.5 without any specifications.

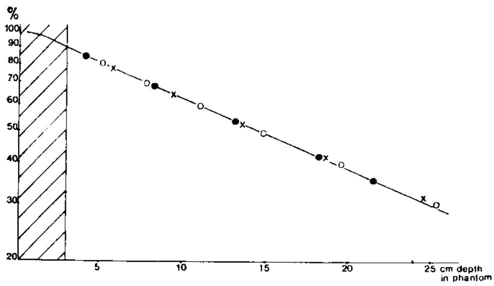

Fig. 11. Central axis depth absorbed dose for ^{60}Co, SSD = 70 cm, 10 cm × 10 cm, ϱ_l = 0.42 g/cm^3. Measured values (○), calculated values using 'absorption equivalent density' 0.51 g/cm^3 and inverse square law correction (×), calculated values using 'effective density' 0.67 g/cm^3 (○).

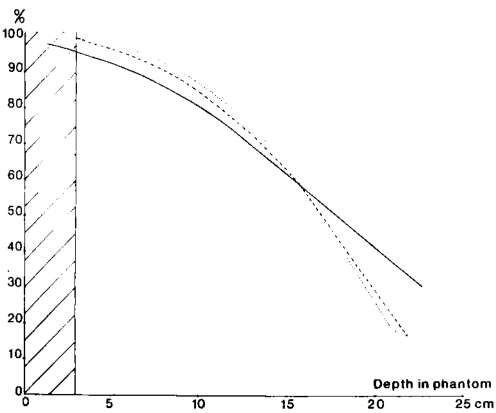

Fig. 12. Central axis depth absorbed dose for 35 MeV e$^-$, SSD 110 cm, 10 cm × 8 cm, ϱ_l = 0.42 g/cm^3, d = 0.64 g/cm^3, d′ = 0.67 g/cm^3. Full-drawn curve indicates measured, dashed curve calculated values using 'absorption equivalent density' and inverse square law correction, dotted curve calculated values using 'effective density' (d′) for ^{60}Co and SSD 70 cm.

Clinical application

Cobalt-60. The investigation shows that the correction of depth absorbed dose data for water when applied to lung tissue can be done by adjusting to depth in g/cm^2 and (1) using an 'absorption equivalent density' followed by a separate inverse square law correction, or, (2) using an 'effective density' which already includes inverse square law correction for the valid focus distance (Fig. 11).

Fig. 5 shows that even the distribution perpendicular to the central axis is retained by this method. This method thus permits the transformation of an isodose-diagram as a whole into a cross section of the patient. Fig. 6 also shows that the correction can take place with sufficient accuracy parallel to the central axis, and not along lines of divergence with sufficient accuracy for SSD $\geqslant$ 70 cm.

The procedure for drawing a corrected isodose diagram according to alternative (2) is, then, as follows: A number of lines parallel to the central axis and passing through the entire cross section of the patient are drawn at distances one or two centimetres apart. The thicknesses of different materials along these

Table 1

Measured and calculated depth dose values

Calculated depth absorbed dose in % 35 MeV e⁻, SSD 110 cm, 10 cm × 8 cm	Measured depth absorbed dose		
	$\varrho_l = 0.58$ g/cm³	$\varrho_l = 0.42$ g/cm³	$\varrho_l = 0.32$ g/cm³
From 'absorption equivalent density' and inverse square law correction			
90	86	86	86
80	76	76	76
70	68	68	68
60	60	60	61
50	52	54	55
40	46	48	49
30	39	42	44
20	32	36	38
From 'effective density' for ^{60}Co			
90	85	83	81
80	75	74	71
70	68	66	64
60	60	59	55
50	54	54	52
40	48	48	47
30	42	43	42
20	36	37	37

lines are then determined, each of which is multiplied by the 'effective density', whereby the depths of the border-lines in the cross section measured in g/cm² are obtained. The same lines are drawn in the water isodose diagram to be used, and the depths in g/cm² for the different isodoses (90 %, 80 %, etc.) are read. A comparison along corresponding lines in the cross section of the patient and in the isodose diagram will give the regions of density in which the different isodose curves lie.

The exact point of intersection between an isodose and the line is then determined in the following way: The depth in g/cm² of the border-line nearest the isodose in the direction of the beam entrance is subtracted from the depth in g/cm² of the same isodose. The resulting difference is then divided by the 'effective density' of the region. The quotient is the distance in cm from the

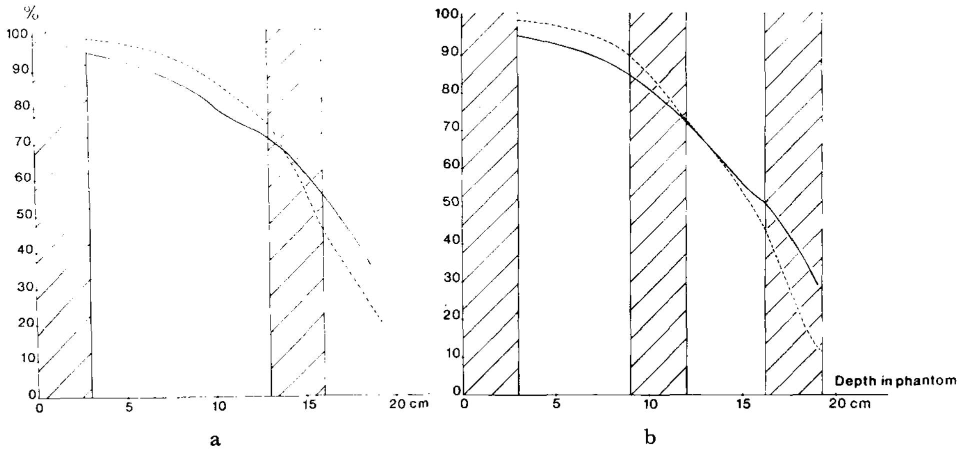

Fig. 13. Central axis depth absorbed dose for 35 MeV e^-, SSD 110 cm, 10 cm × 8 cm, ϱ_l = 0.42 g/cm^3. Full-drawn curve indicates measured, dashed curve calculated values using 'effective density' for ^{60}Co = 0.67 g/cm^3. a) Phantom E. b) Phantom F.

border-line mentioned above to the new point of intersection for this isodose on the line investigated. After having established the intersections of the different isodose curves along all the lines, the complete, corrected isodose diagram can easily be drawn.

35 MeV electrons. Fig. 9 shows that adjusting according to depth in g/cm^2 cannot be done with a constant value of the 'absorption equivalent density' if an agreement along the entire depth absorbed dose curve is wanted. On the other hand it is possible to choose a value which gives the least deviation within the most valid depth interval. The dashed curve in Fig. 12 was obtained at calculation according to the g/cm^2 method with constant value for the 'absorption equivalent density' and afterwards correction for inverse square law. This value was chosen so that measuring curve and calculated curve cross each other at 60 %. The volume weights of 0.32, 0.42 and 0.58 g/cm^3 thus correspond to the 'absorption equivalent densities' of 0.60, 0.64 and 0.72 g/cm^3, respectively (giving a correct 60 % depth absorbed dose), that is essentially higher than for ^{60}Co.

Correction for inverse square law is of much less importance for SSD 110 cm than for SSD 70 cm. This means that the 'effective densities' for ^{60}Co (SSD 70 cm) and 35 MeV electrons (SSD 110 cm) ought to be more comparable. The 'effective densities' for ^{60}Co and for corresponding volume weights are 0.60, 0.67 and 0.76. If these values are used as the 'effective density' for electrons,

Table 2

Deviations between calculated and measured depth absorbed doses

Calculated depth absorbed dose in % 35 MeV e$^-$, SSD 110 cm, 10 cm × 8 cm, ϱ_l = 0.42 g/cm^3, using 'effective density' 0.67 g/cm^3 for ^{60}Co:	Measured depth absorbed dose in	
	Phantom E	Phantom F
90	84	85
80	74	78
70	69	70
60	63	61
50	58	59
40	50	49
30	41	43
20		36

curves are obtained which for practical purposes show the same approximate agreement with measuring values as those described earlier (Fig. 12).

The calculated curves show the greatest divergence from the measurement curves close to the thorax wall as well as at greater depths in the lung tissue (Table 1). The relative deviation near the bordering surface is relatively low, but after the normalizing point of 60 % it increases.

Fig. 13 shows measured depth absorbed doses calculated according to depth in g/cm^2 using 'effective density' for ^{60}Co in the phantoms E and F in Fig. 1 b. Table 2 gives deviations between calculated and measured depth absorbed dose in figures. The comparison between Tables 1 and 2 reveals that the deviations are of the same magnitude.

The measured absorbed dose distribution perpendicular to the central axis in lung tissue shows relatively good agreement with the absorbed dose distribution in water equivalent material at the levels which in the approximate depth correction are to agree to the depths in lung tissue (Fig. 10). The measured central depth absorbed doses at the two valid depths were established = 100 %. There is complete agreement only for depths having central axis depth absorbed dose of 60 %. Thus, a normalization at central axis for the measured curve gives 104 and 108 %, respecetively, for the calculated curves in the central axis.

Within the limits of error which are seen in Tables 1 and 2, the electron isodoses for SSD 110 cm can be transformed in their entirety parallel to the central axis, according to the method given on page 123, using 'effective density' measured for ^{60}Co and SSD 70.

A few patients were irradiated with a lateral electron field. The measurement values obtained in the oesophagus show a good agreement with the calculations done in accordance with the above principle.

The importance of this simplified isodose-correction for electrons from the viewpoint of dosage will be illustrated by two examples.

One field. Assumed that the relevant absorbed dose is 90 %, that is, the area to be irradiated is between 80 and 100 %, the following deviation is obtained for 6 000 rad and a fairly dense lung tissue with a volume weight of 0.42 g/cm^3: The absorbed dose within the treatment area, calculated according to the method just mentioned, lies between 5 330 and 6 670 rad, that is, the minimal figure lies 400 rad lower than was calculated. At a depth of 15 cm, the calculated absorbed dose is 4 270 and the true one 4 130, a deviation of 140 rad. On the other hand, the calculated absorbed dose at 18 cm depth is 2 810, but the true one is 3 310, an error of 500 rad. If no correction of water absorbed dose data is done at all, the error at these two depths would, however, fall at about 3 000 rad. If there is a dense middle wall within the lung tissue, the deviations are largely the same as in the previous case.

Two opposing fields. A distance between both the opposite entry portals of 20 cm is assumed with 14 cm lung tissue between the lung walls. The calculated absorbed dose summed from both of the fields differs within the entire area with ± 8 %, from the true absorbed dose, except for a centimetre close to the surface, where the calculated dose is 15 % too low. If there is a dense middle wall within the lung tissue, the figures are somewhat lower, being then 5 and 10 %, respectively.

Conclusions

The dose absorbed in the tumour and in the healthy tissue of a patient must be as accurately established as possible. Corrections for inhomogeneity are therefore necessary in dose planning programmes. The method described in this paper has been used routinely in our department since 1967 for normal planning, mainly performed by radiographers. It will be transferred to our programme for automatic dose planning, which is under development.

The investigation has proved that this simple method gives sufficiently accurate results for clinical purposes for both ^{60}Co gamma and electron beam therapy. For electrons there will still remain a certain small discrepancy between true and calculated values, which, however, is quite acceptable in comparison to the errors obtained without any corrections.

Clinical measurements of 'absorption equivalent density' also make it possible to estimate the true lung volume weight of a patient from the phantom data presented in this paper.

SUMMARY

A simple method for the construction of individual isodose curves in lung tissue for ^{60}Co and 35 MeV electrons is described. The validity of the method was experimentally verified. A mean volume weight for normal lung tissue was determined for 13 patients.

ZUSAMMENFASSUNG

Eine einfache Methode, individuelle Isodosiskurven im Lungengewebe für ^{60}Co und 35 MeV Elektronen zu konstruieren, wird beschrieben. Die Gültigkeit der Methode wurde experimentell nachgewiesen. Ein mittleres Volumengewicht des normalen Lungengewebes von 13 Patienten wurde bestimmt.

RÉSUMÉ

Description d'une méthode simple pour la construction de courbes isodoses individuelles dans le tissu pulmonaire pour le ^{60}Co et pour les électrons de 35 MeV. La validité de cette méthode a été vérifiée expérimentalement. L'auteur a déterminé pour 13 malades un volume-poids moyen pour le tissu pulmonaire normal.

REFERENCES

1. Almond P. R., Wright A. E. and Boone M. L. M.: High-energy electron dose perturbations in regions of tissue heterogeneity, Part II: Physical models of tissue heterogeneities. Radiology 88 (1967), 1146.
2. Boone M. L. M., Almond P. R. and Wright A. E.: High-energy electron dose perturbations in regions of tissue heterogeneity. Ann. N. Y. Acad. Sci. 161 (1969), 214.
3. Dahl O. and Vikterlöf K. J.: Den fungerande människolungans röntgenabsorption; en undersökning med sikte på djupdosberäkningar och fantomkonstruktioner. (In Swedish.) Nord. Med. 54 (1955), 1576.
4. Dahler A., Baker A. S. and Laughlin J. S.: Comprehensive electron-beam treatment planning. Ann. N. Y. Acad. Sci. 161 (1969), 198.
5. Depth dose tables for use in radiotherapy. Brit. J. Radiol. (1961) Suppl. No. 10.
6. ICRU Report 10d: Clinical dosimetry. NBS Handbook No. 87, National Bureau of Standards, Washington 1963.
7. Laughlin J. S.: Symposium on high-energy electrons, Montreux 1964, p. 262. Proceedings, Springer, Berlin 1965.
8. — High energy electron treatment planning for inhomogeneities. Brit. J. Radiol. 38 (1965), 143.
9. Leung P. M. K., Seaman B. and Robinsson P.: Low-density inhomogeneity correction for 22 MV X-ray therapy. Radiology 94 (1970), 449.
10. Pohlit W.: Calculated and measured dose distributions in inhomogeneous materials and in patients. Ann. N. Y. Acad. Sci. 161 (1969), 189.
11. Sundbom L.: Dose planning for irradiation of thorax with ^{60}Co in fixed-beam teletherapy. Acta radiol. Ther. Phys. Biol. 3 (1965), 343.